Development and testing of a frequency-agile optical parametric oscillator system for differential absorption lidar

Weibring, Petter; Smith, JN; Edner, Hans; Svanberg, Sune

Published in:
Review of Scientific Instruments

DOI:
10.1063/1.1599065

2003

Development and testing of a frequency-agile optical parametric oscillator system for differential absorption lidar

P. Weibring, J. N. Smith,[a] H. Edner,[b] and S. Svanberg
Department of Physics, Lund Institute of Technology, S-221 00 Lund, Sweden

(Received 23 July 2002; accepted 11 June 2003)

An all-solid-state fast-tuning lidar transmitter for range- and temporally resolved atmospheric gas concentration measurements has been developed and thoroughly tested. The instrument is based on a commercial optical parametric oscillator (OPO) laser system, which has been redesigned with piezoelectric transducers mounted on the wavelength-tuning mirror and on the crystal angle tuning element in the OPO. Piezoelectric transducers similarly control a frequency-mixing stage and doubling stage, which have been incorporated to extend system capabilities to the mid-IR and UV regions. The construction allows the system to be tuned to any wavelength, in any order, in the range of the piezoelectric transducers on a shot-to-shot basis. This extends the measurement capabilities far beyond the two-wavelength differential absorption lidar method and enables simultaneous measurements of several gases. The system performance in terms of wavelength, linewidth, and power stability is monitored in real time by an étalon-based wave meter and gas cells. The tests showed that the system was able to produce radiation in the 220–4300-nm-wavelength region, with an average linewidth better than 0.2 cm^{-1} and a shot-to-shot tunability up to 160 cm^{-1} within 20 ms. The utility of real-time linewidth and wavelength measurements is demonstrated by the ability to identify occasional poor quality laser shots and disregard these measurements. Also, absorption cell measurements of methane and mercury demonstrate the performance in obtaining stable wavelength and linewidth during rapid scans in the mid-IR and UV regions. © *2003 American Institute of Physics.* [DOI: 10.1063/1.1599065]

I. INTRODUCTION

With the growing awareness of the serious environmental impact of certain industrial activity, and more stringent regulations on emissions, the need for powerful measurement techniques for air pollutant emission is increasing. Optical remote sensing techniques are particularly advantageous, allowing large-area monitoring and avoiding sample extraction and preparation difficulties.[1] Three-dimensional measurements can be performed with the lidar technique, by using pulsed lasers and detecting the backscattered light from molecules and aerosols in the atmosphere in a radar-like mode. If the wavelength of the laser is varied from an absorption line of a certain gas to a nearby wavelength position with less absorption, the detected changes in the backscattered light intensity can be used to evaluate the gas concentration profile along the laser beam. This technique, called differential absorption lidar (DIAL), is operational for many pollutants and several mobile DIAL systems have been developed.[2,3] The ability to remotely measure the flux of a specific gas from different sources is particularly useful. This is achieved by combining wind data with a mapping of the concentration distribution in a vertical section downwind from the source.[4] In this way, several sources can be studied and the total pollutant flux from an industrial area can be measured.

The laser source in a DIAL system optimized for monitoring of several different gases must be tunable over a large spectral region. Many systems have been based on dye lasers, which can cover the entire visible region with different dyes. However, each dye is normally limited to a rather small spectral interval and a larger wavelength switch requires cleaning and dye changes. In addition, some dyes are not stable over longer laser runs and have to be frequently exchanged. These procedures severely hamper the possibilities of measurements of more than one species at a time. Thus, an all-solid-state laser system that can be rapidly and continuously scanned in different wavelength regions would be much preferred. One approach is to use a Ti:sapphire laser system, tunable in, e.g., the 700–1000 nm region, which can be extended using frequency doubling and tripling. The drawback is the broad linewidth, which can be handled for specific wavelengths by injection seeding.[5] A larger and nearly continuous tuning range can be produced with an optical parametric oscillator (OPO) laser system, which has been investigated in this study. An OPO system pumped by a frequency-tripled Nd:YAG laser can be tuned from 440 to 1800 nm with the signal and idler output, and the region covered can be expanded to 220–4300 nm with frequency doubling and mixing techniques.

The capability of rapid and accurate wavelength scanning is critical in a DIAL system based on a single laser

[a]On leave from: Department of Environmental Engineering Science, California Institute of Technology, Pasadena, CA 91125; present address: Atmospheric Chemistry Division, National Center for Atmospheric Research, P.O. Box 3000, Boulder, CO 80307.
[b]Electronic mail: hans.edner@fysik.lth.se

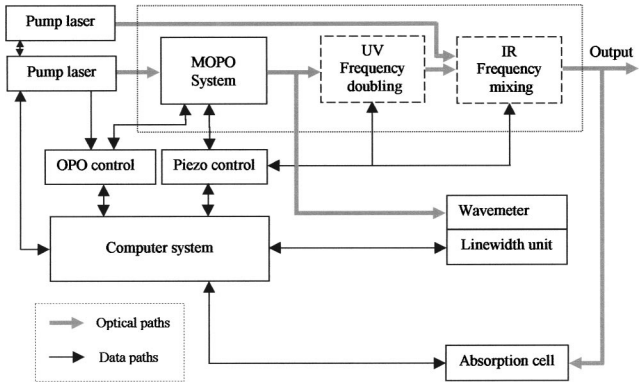

FIG. 1. Schematic view of the lidar transmitter, control, and diagnostic systems. The transmitter (dotted box) consists of an OPO, and doubling and difference frequency generation stages, which are pumped by two Nd:YAG pump lasers. The real-time diagnostic and calibration system consists of a Fabry–Pérot interferometer and a multigas absorption cell system. All functions are controlled by a personal computer using software written in the LabVIEW programing language.

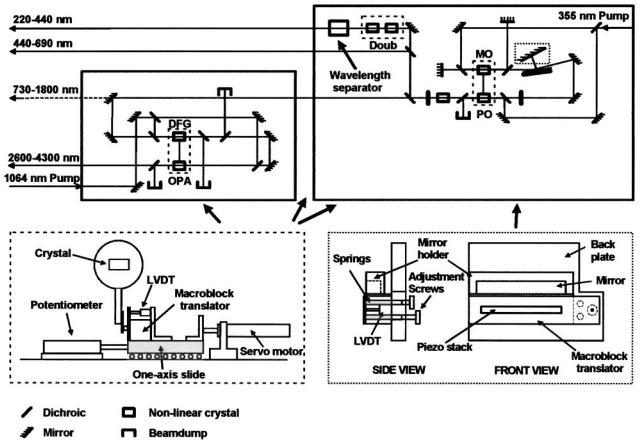

FIG. 2. Optical arrangement for the modified optical parametric oscillator (OPO) and the mixing unit. The upper-right part of the figure shows a layout of the OPO. It consists of a Littman cavity (MO), creating narrow band photons, which are seeded into an instable cavity (PO), generating high output power. The output radiation can either be sent out directly or frequency doubled in an integrated doubling stage. The upper-left part of the figure shows the mixing unit consisting of a difference frequency generation (DFG) stage, followed by an optical parametric amplifier (OPA) stage. To enable fast tuning the Littman cavity mirror in the OPO is modified according to the lower-right part of the figure while all crystal holders are modified according to the lower-left part of the figure.

source. In a two-wavelength DIAL measurement the different wavelengths must be produced in alternating laser shots in order to minimize the noise due to atmospheric turbulence (large-scale movements in the aerosol distribution). In a commercial OPO system the wavelength is changed by moving the tuning mirror and crystal angle with stepper motors, which are too slow for this purpose. One way to achieve a rapid tuning within a smaller region is to seed the OPO with an additional laser source, such as a diode laser.[6,7] However, it is difficult to use this technique in several wavelength regions. We have chosen to modify a commercial OPO system with piezoelectric transducers mounted on the wavelength-tuning mirror, the crystal angle tuning element, and frequency-mixing/doubling stages. All these elements are now actively positioned by a fast feedback system with a sensitive position sensor. This approach also enables the use of a rapid-switching multiwavelength DIAL scheme with more than two wavelengths. This is often necessary for accurate determination of the concentration of different compounds in a mixture. In certain IR regions there is also interference due to H_2O and CO_2 bands, which can make the normal two-wavelength DIAL method difficult to apply. Measurements of hydrocarbon mixtures in the IR are particularly challenging due to overlapping spectral features and interference with water. In these cases, DIAL measurements can advantageously be combined with multivariate statistical techniques in order to separate the contributions from individual species.

II. SYSTEM DESCRIPTION

A diagram of the fast-tuning lidar transmitter is presented in Fig. 1. The main components include a Nd:YAG pump laser, an OPO, and optional doubling and difference frequency generation stages depending on the wavelength required. Two real-time diagnostic and calibration systems are included: a Fabry–Pérot interferometer and a multigas absorption cell system. All functions are controlled by a personal computer using software written in the LabVIEW programing language.[8]

The pump lasers are two Spectra Physics GCR-290 injection seeded Nd:YAG lasers, with a linewidth of <0.003 cm^{-1} and a pulse repetition rate of 20 Hz. The output energy is 1800 mJ at 1064 nm, and after passing through a harmonics generator the output is 500–600 mJ at 355 nm. One of the lasers, which is beam and divergence locked, is used to pump the OPO system and the other one is used as a pump source in the difference frequency generation (DFG) of IR radiation in the 3–4-μm-wavelength region.

The OPO is based on a commercial Spectra Physics MOPO 730,[9] which with the frequency-tripled Nd:YAG laser pump produces tunable radiation in the 440–690 nm (signal) and 730–1800 nm (idler) regions with a pulse energy of up to 100 mJ. The OPO uses β-barium borate (BBO) crystals. A control unit is included that handles all basic functions, such as making large wavelength shifts, providing energy readout and setting up calibration tables for crystal angles. The OPO has been redesigned with piezoelectric transducers mounted on the wavelength tuning mirror in the master oscillator cavity and on the crystal angle tuning element in the master and power oscillator cavities, as shown in Fig. 2. The piezoelectric transducers (Physik Instrumente; Waldbronn) are mounted in such a way as to leave the original state of the OPO unchanged when the piezoelectric controller is switched off. To allow high short- and long-term stability and absolute wavelength accuracy, the piezoelectric transducer on the tuning mirror is actively positioned by a feedback system consisting of a linear variable differential transformer (LVDT) position sensor. A maximum wavelength change of 160 cm^{-1} can be induced by the piezoelectric system in <20 ms. The absolute positioning of the mirror has an uncertainty of 0,02 cm^{-1}, corresponding to 10% of the OPO linewidth. Also, the crystal angles are actively controlled by a similar system as for the tuning mirror to allow

high-power stability and fast wavelength tuning. The acceptance angle of the BBO crystal, determining the demands for crystal readjustment, is approximately 0.3 mrad cm or greater depending on the wavelength region, and the closeness to the degeneracy point. Thus, the needed accuracy for the positioning of the crystals is not as critical as the positioning of the tuning mirror.

To produce radiation in the wavelength range of 2600–4300 nm, the idler output at 1370–1800 nm is mixed with the Nd:YAG fundamental at 1064 nm in a difference frequency generation unit (see Fig. 2). The 1064 nm beam is either produced from the residual from the pump laser, or from a separate Nd:YAG laser. In the latter case a time delay unit synchronizes the firing of the two lasers. The DFG mixing unit is built up of two 35-mm-long $LiNbO_3$ crystals working in series, mounted in such a way that beam displacement caused by the rotation of one crystal is compensated for in the other. Also, by using two crystals, walk-off effects in the phase matching process could be partly compensated. The phase matching angle is controlled by a stepper motor system for large movements and an active piezoelectric system, similar to that described above, for creating small, rapid movements. In the first mixing crystal, radiation from the OPO idler beam is mixed with the 1064 nm resulting in a DFG of radiation in the region around 2600–4300 nm. The depleted 1064 nm beam and the primary idler radiation are split off the beamline. Only the generated 2600–4300 nm radiation then passes through a second $LiNbO_3$ crystal where optical parametric amplification (OPA) with a fresh 1064 nm beam gives an energy output of up to 20 mJ at 2600–4300 nm. The doubling stage inserted in the OPO is also modified by piezoelectric transducers, which enables rapidly tunable radiation in the 220–440-nm-wavelength region with an energy output of up to 12 mJ, either by doubling the signal or the idler from the OPO in a BBO crystal.

The entire system, which includes communication with the OPO and piezoelectric transducer controller, online diagnostics, and data acquisition system, is controlled by three personal computers. A calibration procedure was developed for optimizing the positioning of the piezoelectric transducers at each wavelength in the piezocontrolled scan range (i.e., 160 cm^{-1}). It allows for minor (vertical) displacements of the pump beam, due to temperature-induced expansions in mirror holders, etc., to be compensated for without a need for time-consuming realignment. This calibration procedure results in a linear wavelength–voltage relationship for each transducer, and completes the task in less than 20 s without user intervention. The procedure can be run in an automatic recalibration mode, which is triggered on time, temperature, or output power parameters. The operator can control wavelength, number of shots, order in the wavelength selection, etc., for the measurement with a user interface such as shown in Fig. 3. Displayed are the absorption spectra of some species of interest obtained from a database[10] to aid in the wavelength selection.

Due to the amplification profile of the Littman cavity in the OPO, several modes are allowed to be amplified at the same time, and due to quantum fluctuations in the BBO crystal, the mode quality of the emitted light is a convolution of

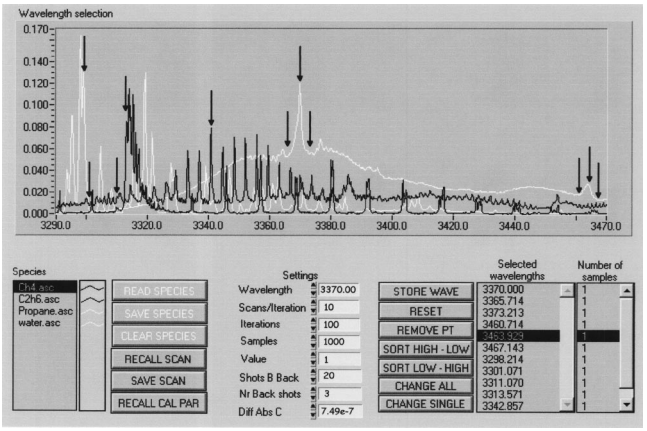

FIG. 3. Measurement and wavelength selection menu from where the operator can control wavelength, number of shots, order in the wavelength selection, averaging type, etc. Displayed are the absorption spectra of some hydrocarbon species obtained from a database, providing aid in the wavelength selection.

randomly amplified modes. The result is pulses with a range of linewidths from 0.07 to 0.4 cm^{-1}, with an average of less than 0.2 cm^{-1}. This does not present a problem when the absorption profiles of the species of interest are broad compared to the emitted radiation. However, for some trace gases there is a need for a linewidth less then 0.2 cm^{-1}, or at least a good control of the actual linewidth of the laser pulses emitted during the measurement. To address these issues, online diagnostic and calibration systems have been implemented, which monitor wavelength, linewidth, and power in real time. If preestablished requirements are not met for a specific pulse, the system discards the corresponding collected data and repeats the measurement until the requirements are fulfilled. The system can alternately allow the collected data to be categorized according to their linewidth. In this way changes in the effective absorption coefficient can be compensated for without losing any shots. The two diagnostic systems used are a wave-meter system and a multigas absorption cell system.

Since the linewidth and wavelength stability are primarily determined by the performance of the OPO, the OPO signal output (440–690 nm) is monitored in real time, by a wave meter (Burleigh, WA-4500). The wave meter incorporates an internal calibration system using a frequency-stabilized HeNe laser allowing a relative accuracy of ± 0.02 cm^{-1}. This accuracy can be turned into an absolute value if the wave meter is recently calibrated by external sources in the appropriate wavelength region. The measurement of linewidth is performed in the software by transferring the étalon signal to a data acquisition card inside the PC. An algorithm has been written to isolate each successive order of the Airy distribution pattern and characterize each in terms of the number of modes and the overall width of the pattern. In the case of single mode output of the laser, each order of the Airy distribution corresponds to a single peak in the étalon pattern and the linewidth measurement is straightforward. If multiple modes are present then the measurement is complicated by the ambiguous definition of linewidth under such conditions. An algorithm was developed in which the total

integrated peak area in a given spectral order is computed and an equivalent Gaussian profile assigned with the same peak intensity and integrated area. The full width at half maximum of this ''equivalent Gaussian'' is then used for calculating a characteristic linewidth.

A second online calibration system was implemented consisting of a set of interchangeable absorption cells containing gases of known concentration that are introduced into a split-off portion of the output beam.[11] This allows measurement of the absorption cross section with every laser shot and enables the possibility to correct deviations in wavelength and linewidth. Since the calibration gas concentration is known, then its absorption at any given wavelength can be directly compared to the atmospheric measurement to improve the quantification of atmospheric gas concentrations. A small portion of the beam is directed into the unit, and is automatically attenuated by a neutral density filter wheel to an appropriate level to insure linearity of the detector. The beam is then divided into a signal and reference beam according to standard practice in absorption cell measurements. The gas cells can be automatically exchanged by rotating the mount when measuring different species. Also, the detectors are automatically exchanged when measuring in different wavelength regions. This system can also be used for accurate wavelength calibration of the OPO wavelength if gases with accurately known peaks are available in the chosen wavelength region.

III. SYSTEM PERFORMANCE

To verify the system performance, the same Burleigh wave meter described earlier was utilized. The wavelength measurement is performed immediately following each shot and transferred to a computer via an RS232 interface. The measurement of linewidth, which the wave meter does not perform in real time, is performed in LabVIEW software by transferring the étalon signal from the wave meter to a second PC. The same algorithm as described in the previous section is used for the evaluation of the linewidth. For comparison purposes the Burleigh acquire utility was used allowing 100 sequential shots to be stored and postevaluated in terms of linewidth and wavelength. The comparison between our and the Burleigh algorithm for the linewidth shows a good agreement. All diagnostic information such as the wavelength from the Burleigh system, the linewidth, and the power from our own evaluation system, is merged together and displayed on a computer screen as shown in Fig. 4.

Several tests were performed to determine the performance of the modified OPO system and compare it with the original design.[12] These comprised monitoring of the stability of wavelength, linewidth, and power as a function of time. Both shot-to-shot fluctuations and long-term variations were tested. All of these parameters were validated at three wavelengths in the 440–690-nm-wavelength region to examine the wavelength dependence. Tests were made at both static conditions, with zero and maximum extension, and in dynamic operation of the piezoelectric transducers. In addition to testing the OPO output in the visible wavelength range, the IR-mixing and UV-doubling units were validated

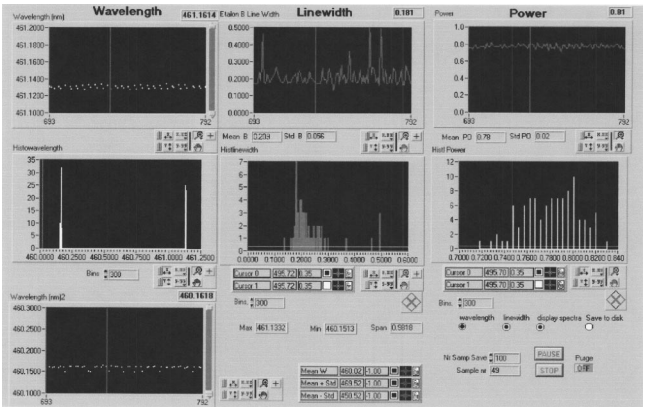

FIG. 4. Realtime data screen dump from the surveillance system. In the upper part, wavelength, linewidth, and power are shown as a function of time. In the lower part, histograms and statistics of the same data are presented.

for pulse energy stability. No direct tests for linewidth and wavelength were performed for these units, since they result from the incoming laser beams that already have been validated. In the place of direct measurements for these units, absorption cell measurements were performed in the IR and UV regions on isolated peaks of methane and mercury in order to infer wavelength and linewidth stability and accuracy.

The performance tests were divided up in several sections in order to understand the impact of both the mechanical modifications and associated electrical control systems on overall performance. The tests were performed for the *original design*, *static operation*, and *dynamic operation*. The complete modified system was tested without the piezosystems turned on, which is refereed to as *original design*. The reason for this denotation is that it was concluded that the mechanical modifications between the unmodified and the modified systems did not effect the performance. Also, a lot of realignment would have been required between tests if the mechanical setup of the unmodified system had to be reinitialized for every wavelength. The *static operation* tests were performed with the piezoelectric controller and system control computer turned on, applying a nonzero voltage on the piezoelectric transducers. In the *dynamic operation* tests the piezoelectric transducers performed a 1-nm-wavelength shift between each shot. The tests for the IR-mixing and UV-doubling units were limited to energy stability according to the procedures described above. Due to the large amount of data, we choose to present only the most critical parts in diagrams.

Figure 5 shows short-term comparisons of (a) wavelength, (b) linewidth, and (c) output power characteristics between the original design and the modified design when it is undergoing a wavelength shift of 1 nm between each shot. In every comparison, the *original design* is shown to the left and the modified to the right. In the upper left of each figure, 100 sequential shots for the original design are shown and in the upper-right part 100 shots at 454.290 nm and 100 shots at 453.237 nm are shown. Each point in the figures represents one laser pulse. In the lower part, histogram comparisons of the same data are presented.

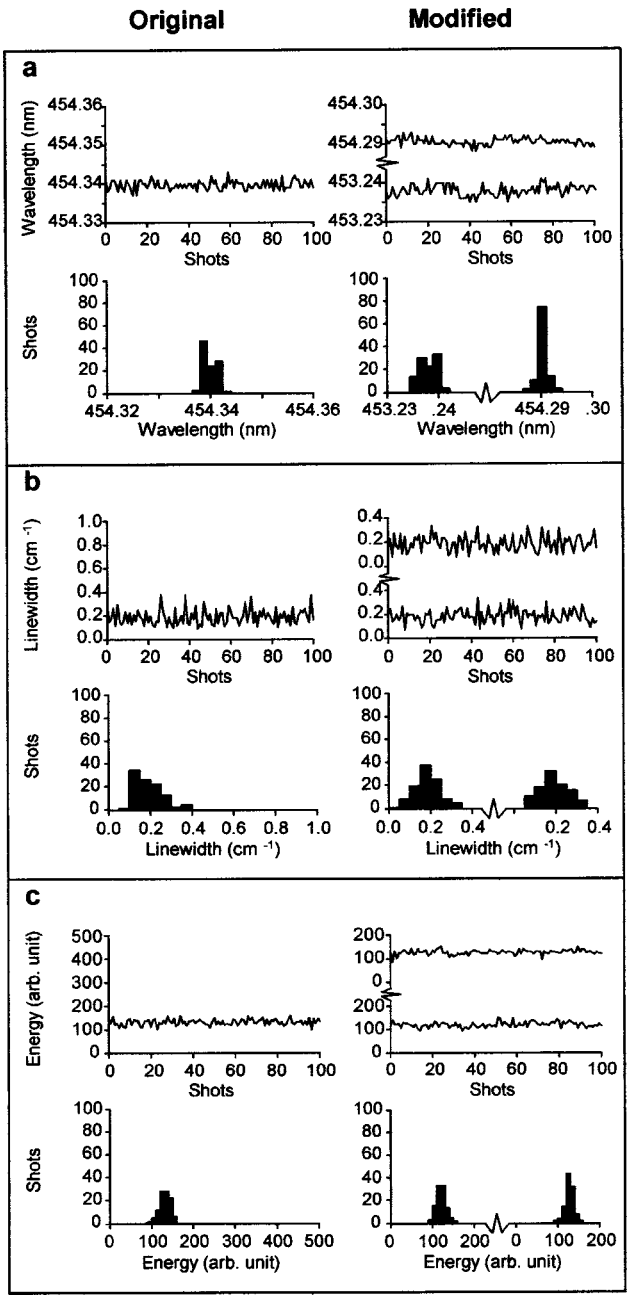

FIG. 5. Short-term comparison between original and modified system of (a) wavelength, (b) linewidth, and (c) output power characteristics between the original design and the modified design when it is undergoing a wavelength shift of 1 nm between each shot. In every comparison, the *original design* is shown to the left and the modified to the right. In the upper left of each figure, 100 sequential shots for the original design are shown and in the upper-right part 100 shots at 454.290 nm and 100 shots at 453.237 nm are shown. Each point in the figure represents one laser pulse. In the lower part, histogram comparisons of the same data are presented.

Figure 6 shows a 4-min-long-wavelength performance test of the modified design, when it is undergoing the same wavelength shift as above and where each point in the figure represents 100 averaged laser shots. The results for the same tests of linewidth and energy stability are presented in Table I. The difference in wavelength between zero voltage of the piezostack and the original design is due to a slight offset that is applied onto the piezostack at zero control voltage, which is necessary for keeping the spring tension constant.

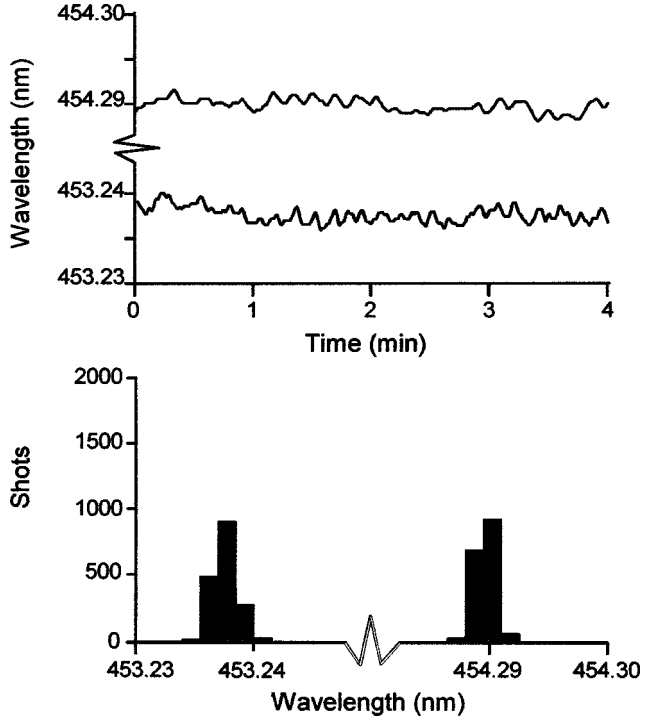

FIG. 6. Four minute wavelength stability measurement of the modified system, when it is undergoing a wavelength shift of 1 nm between each shot. Each point in the upper figure represents 100 averaged laser shots. In the lower part, a histogram of the same data is presented.

The results of the UV and IR mixing tests are included in the lower part of Table I, which presents the energy measurements averaged over a 4 min period in addition to shot-to-shot fluctuations. The incoming mixed wavelengths were 1624.26 and 1064 nm, corresponding to an output wavelength of 3084.65 nm, and 1637.87 and 1064 nm, corresponding to an output wavelength of 3036.75 nm. As can be seen in Table I, the performance of the system in the switching mode corresponds well to the original design. In reviewing the results of the different tests over the whole wavelength region, no significant difference between the original design and the modified one can be detected. The change in linewidth between close-lying wavelengths is explained by the fact that, for even small differences in wavelength, movement of the tuning mirror angle can cause the circumstances for the amplification process in the master oscillator to change. A lower gain profile, for example, will lower the linewidth of the laser light by allowing fewer laser modes to reach laser threshold. During the tests it was found out that by mismatching the tuning mirror angle and the master oscillator (MO) crystal acceptance angle slightly, keeping the power oscillator (PO) crystal at the correct orientation with respect to the tuning mirror, the linewidth could be decreased in a controlled way. This narrowed linewidth did not significantly affect the energy level in the wavelength regions where little seeding of the PO oscillator is needed (i.e., the blue region). In the red wavelength region the linewidth could be decreased but at a cost of less energy output. Energy differences between the tests for the same ''wavelength'' are due to long-term changes in pump laser energy and the fact that the Burleigh wave meter had to be realigned

TABLE I. Test results of wavelength, linewidth, and power stability for different wavelength regions during a 4 min period of time: 1: original design; 2: static operation (piezosystem turned on and control computer connected but no wavelength shift); and 3: dynamic operation (piezosystem turned on and control computer connected inducing a 1-nm-wavelength shift between each laser shot).

	Wavelength		Linewidth		Energy		
Test	Average (nm)	St. dev. (nm)	Average (cm^{-1})	St. dev. (cm^{-1})	Average (arb. unit)	St. dev. (arb. unit)	Shot to shot (%)
1	454.340	0.001	0.19	0.07	147	17	9
2	454.334	0.001	0.16	0.05	117	19	14
3 (WL1)	454.290	0.001	0.19	0.07	119	12	9
3 (WL2)	453.237	0.001	0.19	0.06	120	11	8
1	494.731	0.002	0.15	0.07	220	20	13
2	494.729	0.002	0.14	0.07	177	14	7
3 (WL1)	494.922	0.001	0.15	0.06	280	25	11
3 (WL2)	493.904	0.002	0.13	0.06	221	28	15
1	659.063	0.002	0.12	0.05	121	19	13
2	659.064	0.002	0.12	0.05	102	19	16
3 (WL1)	659.062	0.002	0.11	0.05	121	16	17
3 (WL2)	658.385	0.002	0.11	0.06	85	18	15
1	253.399	n.a.	n.a.	n.a.	133	15	15
3 (WL1)	252.399	n.a.	n.a.	n.a.	131	20	19
3 (WL2)	252.650	n.a.	n.a.	n.a.	134	9	8
1	3084.67	n.a.	n.a.	n.a.	44	8	12
3 (WL1)	3084.67	n.a.	n.a.	n.a.	45	11	15
3 (WL2)	3036.75	n.a.	n.a.	n.a.	38	9	15

between tests. The energy values are consistent for the different setups and wavelength regions.

A critical second test was performed using the absorption in a methane cell with the wavelengths selected to match sharp peaks in the absorption spectrum. In Fig. 7, the selected wavelengths are indicated in the experimentally recorded spectrum of methane. The lower part of Fig. 7 shows the absorbance at the marked wavelengths as a function of time. Every point corresponds to an average of ten cycles, with one shot at each wavelength in one cycle. The results show that the system is able to emit a wavelength sequence with a good precision. No indication of degradation of the original OPO performance after the modifications could be found.

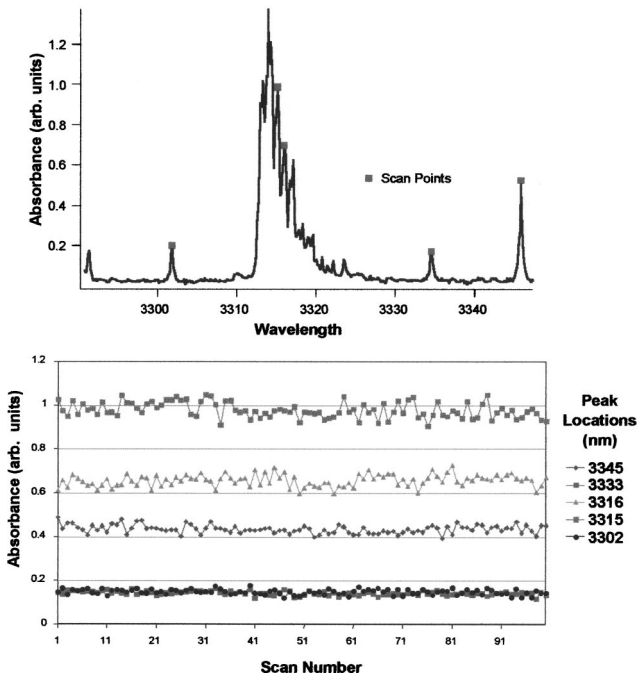

FIG. 7. Scan of five methane peaks in an absorption cell as a function of time. The selected wavelengths are indicated in an experimentally recorded spectrum of methane. The lower part of the figure shows the absorbance at the marked wavelengths as a function of time. Every point corresponds to an average of ten cycles, with one shot at each wavelength in one cycle.

To investigate the influence of the outliers in linewidth a wavelength scan of a separated mercury isotope (^{202}Hg) line was performed at 253.652 nm. The result is shown in Fig. 8, where the absorption profile of mercury is recorded as a function of different linewidths. When performing a mea-

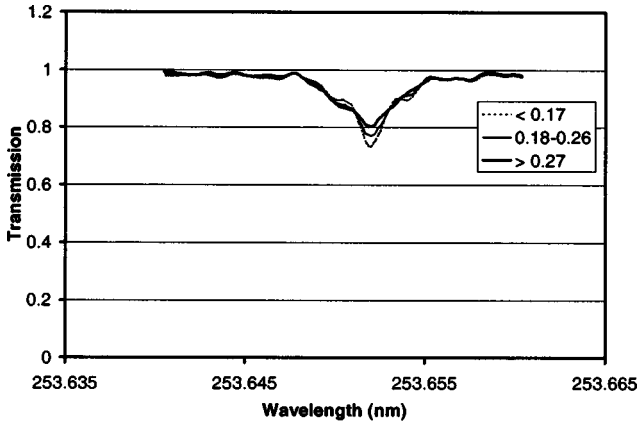

FIG. 8. Wavelength scan of a separated mercury isotope (^{202}Hg) in an absorption cell. Transmission profile is shown as a function of different linewidths.

surement the system measures the actual linewidth of each shot and categorizes and stores the acquired data in the corresponding cross section. When the concentration of a species is evaluated every linewidth category is calculated separately and then summed up with the other linewidth categories. In this way a greater fraction of the shots can be utilized.

IV. DISCUSSION

The fast tuning solid-state lidar transmitter described here extends the measurement capabilities far beyond the standard two-wavelength DIAL method and enables simultaneous measurement of multiple species or resolving interference effects between compounds of interest and background gases such as carbon dioxide or water vapor. Especially in the mid-IR wavelength region there are many hydrocarbons which have overlapping rotational–vibrational transitions that require a multiwavelength approach.

The quantitative identification of multiple, coexisting compounds from their combined spectrum requires not only a measurement system, which has the ability to transmit and detect light at multiple wavelengths, but also the implementation of the right evaluation tools. To manage these requirements, statistical multivariate techniques will be explored. In the field of pollution monitoring, spectrometers have long been used for multiple-species detection, utilizing different multivariate techniques, ranging from multiple linear regression (MLR) to multivariate partial least-squares (PLS) algorithms.[13,14] In these cases, the whole spectral signature, containing hundreds of measurement wavelengths, is utilized for the detection. The whole spectral region could be scanned by a tunable pulsed lidar system, but due to the limited repetition rate of the system, this is not feasible. Here, genetic algorithms in combination with multivariate methods will be explored for reducing the number of measurement wavelengths to the most important ones.

The concept of a multiwavelength mobile lidar system with multivariate techniques and genetic algorithms is attractive for several applications such as the monitoring of petrochemical industries, pipeline leakage detection and surveillance monitoring of diffuse emissions in urban areas. The integration and performance of the new transmitter in a mobile lidar system is discussed in a forthcoming publication.[15]

ACKNOWLEDGMENTS

This work was supported by the Swedish Space Board, The Knut and Alice Wallenberg Foundation, and the Lund/Caltech Academic Exchange Program. The authors want to thank Fredrik Nordin and Ulf Gustafsson for assistance in the construction and testing period. The fruitful cooperation with Spectra Physics, Inc., throughout this project is gratefully acknowledged.

[1] M. W. Sigrist, *Chemical Analysis* (Wiley, New York, 1994), Vol. 127.
[2] H. Edner, P. Ragnarson, and E. Wallinder, Environ. Sci. Technol. **29**, 330 (1995).
[3] D. Weidauer, P. Rairoux, M. Ulbricht, J. P. Wolf, and L. Wöste, in *Advances in Atmospheric Remote Sensing with Lidar*, edited by A. Ansmann, R. Neuber, P. Rairoux, and U. Wandinger (Springer, Berlin, 1996), p. 423.
[4] P. Weibring, M. Andersson, H. Edner, and S. Svanberg, Appl. Phys. B: Lasers Opt. **B66**, 383 (1998).
[5] J. Yu, P. Rambaldi, and J. P. Wolf, Appl. Opt. **36**, 6864 (1997).
[6] M. J. T. Milton, T. D. Gardiner, F. Molero, and J. Galech, Opt. Commun. **142**, 153 (1997).
[7] M. S. Webb, K. B. Stanion, D. J. Deane, W. A. Cook, W. A. Neuman, and S. P. Velsko, Proc. SPIE **2700**, 269 (1996).
[8] M. Andersson and P. Weibring, Lund Report No. LRAP-201, Lund Institute of Technology, Lund, Sweden (1996).
[9] *Quanta-Ray MOPO-730 Optical Parametric Oscillator*, Instruction Manual (Spectra-Physics Lasers, 1995).
[10] *Database and Quantitative Analysis Program for Measurements of Gases, QASoft '96* (Infrared Analysis, Anaheim, CA, 1996).
[11] F. Mellegård, Lund Report No. LRAP-264, Lund Institute of Technology, Lund, Sweden (2000).
[12] F. Nordin, Lund Report No. LRAP-243, Lund Institute of Technology, Lund, Sweden (1999).
[13] K. Esbensen, *Multivariate Analysis*, 5th ed. (CAMO, Oslo, 2001).
[14] P. Geladi and B. R. Kowalski, Anal. Chim. Acta **185**, 1 (1986).
[15] P. Weibring, H. Edner, and S. Svanberg, Appl. Opt. **42**, 3583 (2003).